Diffusivity of simple fluid mixtures in porous media: molecular dynamics simulations and correlation models

Xing Qin [a], Bing-Jian Zhang [a,*], Hui Zhang [a], Wenxuan Hu [b]

[a] *Department of Chemistry, Zhejiang University, Hangzhou 310027, Zhejiang, China*
[b] *Department of Earth Sciences, Nanjing University, Nanjing 210093, China*

Abstract

Equilibrium molecular dynamics simulations have been used to calculate the diffusivity of simple fluid mixtures in macrovolume systems and in porous media at different temperatures, densities, and pore widths. Based on the Chapman–Enskog theory and the Heyes relationships, two correlation models, which can describe the diffusivity of simple fluid mixtures in porous media as a function of the reduced temperature, density, and pore width, are proposed. The validity of the models is evaluated by comparing the calculated diffusivity data with those from the simulation data.
© 2004 Elsevier B.V. All rights reserved.

Keywords: Molecular simulation; Diffusion coefficient; Porous media; Correlation models

1. Introduction

Molecular dynamics (MD) simulation is a very useful method to study the transport properties of fluids including the diffusion coefficient and viscosity. Equilibrium molecular dynamics (EMD) and nonequilibrium molecular dynamics (NEMD) are the two major types of simulation methodologies for studying the transport properties. The EMD and NEMD approaches to transport properties have been reviewed by Cummings and Denis [1]. In recent years, MD simulations have been successfully performed for the investigations of the fluid behavior in macrovolume systems.

But much less work has been reported on the transport processes in fluid/pore systems than in macrovolume systems [2]. The properties of fluids in porous media play an important role in many fields such as the petroleum industry. Due to the complexity of the extreme conditions in such systems, it is quite a difficult task to obtain the experimental data under normal conditions. Computer simulations, especially by MD, are able to simulate the real complicated conditions and give satisfactory results. Bitsanis et al. [3–5] have done much work on it recently. They presented a local

average density model (LADM) for viscosity and diffusivity. The EMD and NEMD simulations were also performed and they found that the diffusivity increases at very small pore widths. However, they concentrated only on one state point that has one temperature and density. In this work, we performed the EMD simulations for the diffusivity of the equal molar mixture of argon and krypton at different reduced temperatures, pore widths, and densities, and proposed two correlation models which describe the diffusivity of simple fluid mixtures in porous media as a function of the temperature, density, and pore width. In continuation of our previous work, these methods have been expanded to the mixture of chain molecular fluids in multilayer silicate and published elsewhere [6–10].

2. Theory

In the last two decades, the transport properties of simple fluids, i.e., hard sphere (HS) and Lennard–Jones (LJ) fluids, have been obtained by MD simulations over the fluid range up to the fluid–solid phase boundary. Chapman–Enskog (CE) theory for the HS transport properties is surprisingly good over most of the fluid range. Heyes [11] has empirically extended the CE theory to liquid densities using

hard sphere MD data. He also applied the CE relationships to the transport coefficients of LJ fluids by attaching a temperature-dependent hard sphere diameter to the LJ molecule.

For a macrovolume system formed by N spherical molecules in volume V and at temperature T, and expressing the potential energy of the studied system as a sum of LJ pair interaction potentials, Heyes' work [11] can be used as follows to obtain the diffusivity of an LJ fluid:

$$\frac{Dm^{1/2}}{V_0^{1/3}T^{1/2}} = \frac{3}{8}\frac{(k_B/\pi)^{1/2}}{2^{1/3}}1.271(X - 1.384), \tag{1}$$

where m is the mass of the molecule, $V_0 = \sigma^3/2^{1/2}$ the volume per particle of the close pack (fcc) solid, σ the hard sphere diameter, D the diffusivity, and $X = V/V_0$ the reduced volume. The temperature-dependent hard sphere diameter is given by

$$\frac{\sigma_{HS}}{\sigma_{LJ}} = a_1 + a_2T^* + a_3T^{*2} + a_4T^{*3} + a_5T^{*4}, \tag{2}$$

where σ_{HS} and σ_{LJ} are the diameters of HS and LJ fluids, respectively, $a_1 = 1.096469$, $a_2 = -0.133393$, $a_3 = 0.0467091$, $a_4 = -0.0077295$, $a_5 = 0.00043227$, $T^* = k_BT/\varepsilon$ is the reduced temperature, and ε the potential parameter.

From Eq. (1) in reduced units we get

$$\frac{D_m^*}{\sqrt{T^*}} = \frac{3}{8}1.271\frac{1}{\sqrt{2\pi}}(X - 1.384)\frac{\sigma_{HS}}{\sigma_{LJ}}, \tag{3}$$

where $D_m^* = D(m/\varepsilon\sigma^2)^{1/2}$ is the reduced diffusivity of LJ fluids in a macrovolume system, and $X = V/V_0 = \sqrt{2}/\rho^*$. Substituting Eq. (2) into Eq. (3), we obtain

$$\frac{D_m^*}{\sqrt{T^*}} = 0.1901\left(\frac{\sqrt{2}}{\rho^*} - 1.384\right)(a_1 + a_2T^* + a_3T^{*2}$$
$$+ a_4T^{*3} + a_5T^{*4}), \tag{4}$$

where $\rho^* = \rho\sigma^3$ is the reduced density. The diffusivity of LJ fluids in macrovolume system can be calculated from Eq. (4).

For an LJ fluid defined as before, but confined between two parallel structured walls, the slit pore width H was defined as the distance between the two wet walls, which means that the structured walls are covered with one layer of fixed atoms and composed of the same particles as the fluids. The reduced diffusivity in porous media D_p^* is the function of the reduced temperature T^*, the reduced density ρ^*, and the reduced pore width $H^* = H/\sigma$. As for a constant H^*, the diffusivity at specific temperature and density is a constant value, the values of the reduced diffusivity in porous media can be shown as $\ln(D_p^*/D_m^*)$. We know that the reduced diffusivity will decrease with an increase in the reduced density and increase with an increase in the reduced temperature in the liquid region, and further, that at very small pore widths, the reduced diffusivity will decrease

with an increase in the reduced pore widths. So, at first we get

$$D_p^* \propto \frac{1}{\rho^*}, \qquad D_p^* \propto T^*, \qquad D_p^* \propto \frac{1}{H^{*n}}, \tag{5}$$

where n is the exponent that will be determined later. But these factors have more obvious and extensive effects on the diffusivity in macrovolume than in porous media. The diffusivities in porous media change with the reduced density and reduced temperature to a lesser extent than in macrovolume. From these relationships, a new correlation model describing the diffusivity of the simple liquid mixtures in porous media can be obtained:

$$\ln\left(\frac{D_p^*}{D_m^*}\right) = A\left(\frac{\rho^*}{T^*H^{*n}}\right) + B, \tag{6}$$

where A and B are the spring constants.

A possible problem with a form such as Eq. (6) is that the ratio $D_p^*/D_m^* \neq 1$ when $H^* \to \infty$, or $D_p^* \neq D_m^*$ when the system changes from porous media to macrovolume. As an improved form of Eq. (6), another similar correlation model can be expressed as follows:

$$\ln\left(\frac{D_p^*}{D_m^*}\right) = \frac{L\rho^{*c}}{T^*}\left(\frac{1}{H^* - 1}\right)^n \tag{7}$$

where L is the spring constant, n and c are the empirical constants.

The ability of these two models, given by Eqs. (6) and (7), to describe the diffusivity of simple liquids in porous media, is needed to calculate the diffusivity D_p^* as a function of T^*, ρ^*, and H^*, and compare with the experimental data or the simulation results. There are no experimental diffusivity data of the liquids in porous media and only a few simulation results about the diffusivity in porous media can be found; moreover, the simulation results deal with just one state point. In this work, the simulation results of diffusivity for a mixture of argon and krypton, both in macrovolume systems and in slit porous media, are presented (Table 1).

Table 1
The simulation results of diffusivity for mixture of argon and krypton in slit porous at different state points

Pore width, H^*	Temperature, T^*	Density, ρ^*	Diffusivity, D^*
9	1	0.3	10.5
10	1	0.3	7.7
10	1	0.2	8.0
10	1	0.4	7.5
10	1	0.5	7.4
10	1.1	0.3	7.8
10	1.2	0.3	7.8
10	1.25	0.3	7.9
12	1	0.3	5.0
14	1	0.3	3.8

All the variables are in reduced units.

We predigest the simple fluid mixtures to simple liquids using the mixing rule. For this reason, Eq. (4) can be used to calculate diffusivities in macrovolume systems.

3. Simulations

The EMD simulations are performed on the LJ 12-6 fluid, for which the potential is

$$u = 4\varepsilon \left[\left(\frac{\sigma}{r} \right)^{12} - \left(\frac{\sigma}{r} \right)^{6} \right], \tag{8}$$

where σ and ε are the potential parameters, r the distance between two particles. For argon we choose $\sigma_{Ar} = 3.405$ Å, $\varepsilon_{Ar}/k_B = 119.8$ K, and for krypton we choose $\sigma_{Kr} = 3.633$ Å, $\varepsilon_{Kr}/k_B = 167$ K.

We use the following mixing rules:

$$\sigma_{12} = \tfrac{1}{2}(\sigma_{Ar} + \sigma_{Kr}),$$
$$\varepsilon_{12} = \sqrt{\varepsilon_{Ar}\varepsilon_{Kr}},$$
$$\sigma = \sqrt[3]{c_{Ar}^2 \sigma_{Ar}^3 + 2c_{Ar}c_{Kr}\sigma_{12}^3 + c_{Kr}^2 \sigma_{Kr}^3}, \tag{9}$$
$$\varepsilon = \frac{c_{Ar}^2 \varepsilon_{Ar}\sigma_{Ar}^3 + 2c_{Ar}c_{Kr}\varepsilon_{12}\sigma_{12}^3 + c_{Kr}^2 \varepsilon_{Kr}\sigma_{Kr}^3}{\sigma^3},$$

where σ_{12} and ε_{12} are the mutual potential parameters of argon and krypton, and σ and ε the potential parameters of simple fluid mixtures. The truncation distance for the potential is chosen to be 2.5σ.

We put the LJ fluid particles into two parallel wet walls, which means that the walls are composed of one layer of the same particles as that of the fluids (see Fig. 1). The fluid–fluid and fluid–wall intermolecular potentials are also identical. The system contains 144 particles: 108 of them are in the fluid form and 18 in each wall. The wall particles are composed of the same number of argon and krypton atoms and arranged in an fcc lattice. The wall particles remain stationary during the process of simulation. The boundary conditions are applied in the x and y directions. The simulation of a new z coordinate for each particle has been described in Ref. [3].

The time step in reduced units is chosen to be 0.00462 (10–14 s). The initial 50 000 time steps are disregarded and the equilibrium MD simulations of 750 000–1 050 000
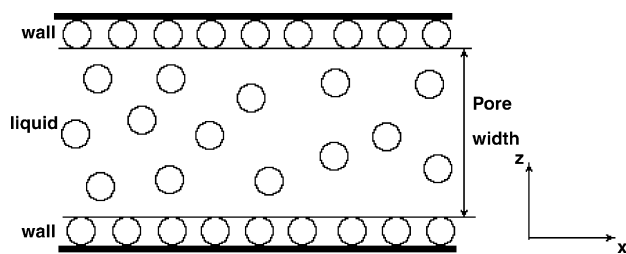
time steps (7.5–10.5 ns) are performed. In the simulations, Verlet's algorithm is used to solve the equations of motion.

The diffusivity is calculated using the Green–Kubo formula,

$$D = \frac{1}{d} \int_0^\infty \mathrm{d}t \, \langle v_1(0)v_1(t) \rangle, \tag{10}$$

where d is the dimensionality. In some cases, d has been taken as 2 in the case of very small pore widths ($H^* < 4$) [12–14]; however, d has been chosen as 3 in silicate ($H^* \approx 10$) [15,16]. In our calculations, the pore width is not very small and a surge in the z direction has been observed in our previous work [10], so, the z direction should not be ignored and d is taken as 3.

The EMD simulations are performed under the following conditions:

- *Condition 1:* Four reduced temperatures $T^* = 1.00, 1.10, 1.20, 1.25$ at the reduced density $\rho^* = 0.3$ and pore width $H^* = 10$,
- *Condition 2:* Four reduced densities $\rho^* = 0.2, 0.3, 0.4, 0.5$ at the reduced temperature ($T^* = 1.00$) and pore width ($H^* = 10$),
- *Condition 3:* Four reduced pore widths $H^* = 9, 10, 12, 14$ at the reduced density $\rho^* = 0.3$ and temperature $T^* = 1.00$.

4. Results

Firstly, the diffusivities in macrovolume systems are calculated by EMD simulations and compared with those obtained by the experimental methods [17,18]. Diffusivities are calculated for saturated argon at different temperatures (see Fig. 2) and for krypton at different densities but at constant temperature (see Fig. 3). Figs. 2 and 3 show that the diffusivity results of the EMD simulations for the macrovolume argon are in good agreement with the experimental data.

Fig. 1. The pore structure in our simulations in which the wall particles have the same size as the liquid particles.
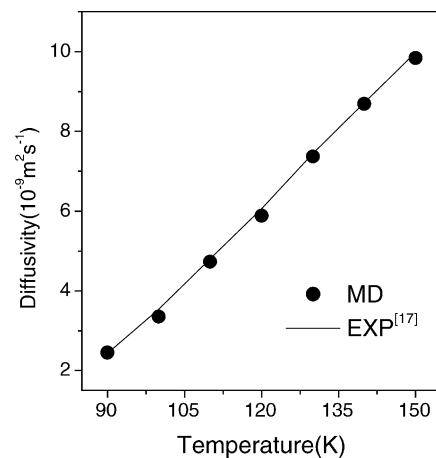

Fig. 2. Diffusivity for saturated argon. (—) Experimental results [17] and (●) our EMD simulation results.
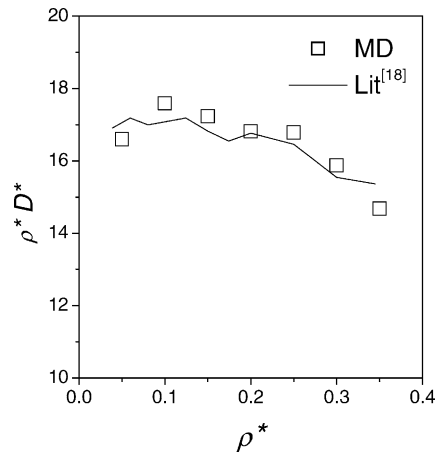
Fig. 3. The coefficient of self-diffusion for krypton at different densities but at constant temperature ($T^* = 1.5$). (—) Simulation data of Michels and Trappeniers [18] and (□) our EMD simulation data.

Secondly, the diffusivities of macrovolume mixtures of argon and krypton are calculated by EMD simulations in order to verify our simulation program further. The simulation results of diffusivities at different compositions are shown in Fig. 4 [19]. The two results are very close. On the other hand, experimental mutual diffusivity for equal molar mixture of argon and krypton is $2.29 \times 10^{-9}\,\text{m}^2\,\text{s}^{-1}$ [20] when the temperature is $115.7\,\text{K}$. The theoretically calculated value is $2.58 \times 10^{-9}\,\text{m}^2\,\text{s}^{-1}$. From this it can be concluded that the mixing rules are correct, and we can regard the mixture as a single fluid, and the program can calculate the diffusivity successfully.

In this section, two temperature-, density- and pore width-dependent models for calculating the diffusivity in porous media are presented. In Eq. (6), the exponent n of H^* had been chosen as 1, 2, 3, and so on. Finally, we found that 2 was the best suited value. So, using the
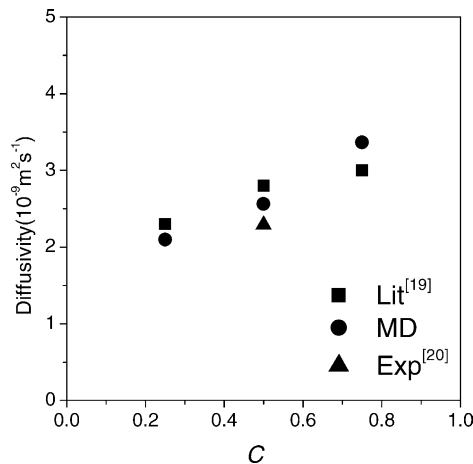

Fig. 4. Diffusivity for mixture of argon and krypton at different constitutive proportions. (■) Simulation result from Ref. [19]; (●) our EMD simulation result; and (▲) experimental data [20].
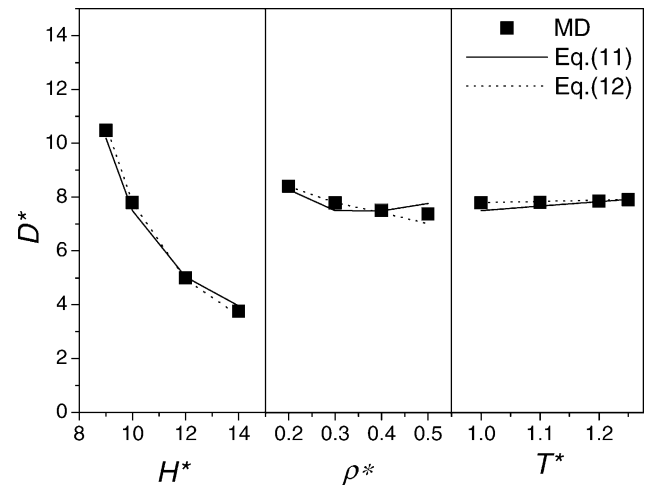

Fig. 5. Reduced diffusivity vs. reduced pore widths, reduced density and reduced temperature. (■) EMD simulation results; (—) result calculated using Eq. (11); and (---) result calculated using Eq. (12).

simulation data shown in Fig. 4 and plotting $\ln(D_p^*/D_m^*)$ versus $T^*/(H^{*2}\rho^*)$, the empirical constants A and B in Eq. (6) was obtained. Eq. (6) now becomes

$$\ln\left(\frac{D_p^*}{D_m^*}\right) = 189.058\left(\frac{\rho^*}{T^{*0.15}H^{*2}}\right) + 0.5052. \tag{11}$$

The data calculated from Eq. (11) are compared with the simulation data (see Fig. 4). The results show that the calculated values are reasonably good.

On the other hand, in Eq. (7), ρ^* and T^* were first assumed to be constant. Using the simulation data shown in Fig. 4, and plotting $\ln[\ln(D_p^*/D_m^*)]$ versus $\ln(H^* - 1)$, the exponent n is found to 1. Similarly, plotting $\ln(D_p^*/D_m^*)$ versus $(T^*/\rho^{*c})(1/H^* - 1)$, the empirical constants L and c in Eq. (7) can be obtained. Eq. (7) now becomes

$$\ln\left(\frac{D_p^*}{D_m^*}\right) = \frac{17.899\rho^{*0.5}}{T^{*0.15}}\left(\frac{1}{H^* - 1}\right). \tag{12}$$

From Eq. (12), the diffusivity of the liquid mixture of argon and krypton in porous media at different reduced temperatures, densities, and pore widths can be calculated exactly. When the reduced pore widths tend to be infinite, the system becomes the macrovolume system, and the right-hand side of Eq. (12) will be zero. Then the diffusivity of liquid mixture in the porous media will be equal to that of macrovolume system. When the pore widths are very small, for example, $H^* \to 1$, then the pore width is equal to the particle's diameter σ and $D_p^* \to \infty$. This situation cannot occur (Fig. 5).

5. Conclusion

MD simulations can provide an insight into the microscopic characters and relate them to the macroscopic

properties. In this work, the diffusivity of a liquid mixture of argon and krypton in slit porous media has been obtained by EMD simulations at different reduced temperatures, reduced densities, and reduced pore widths. Based on the CE theory and the Heyes relationships, the correlation models describing the diffusivity of simple fluid mixtures in porous media as a function of the reduced temperature, reduced density, and reduced pore width are proposed. The results calculated from the models compare well with those from the simulation data.

List of symbols

d	dimensionality
D	diffusivity
D_m	diffusivity in macrovolume system
D_p	diffusivity in pores
H	slit pore width
k_B	Boltzman's constant
m	mass of the molecule
r	distance between two molecules
t	time
T	temperature
u	potential
v	velocity
V	volume

Greek letters

ε	potential parameter
ε_{HS}	potential parameter of HS molecular fluid
ε_{LJ}	potential parameter of LJ molecular fluid
π	ratio of the circumference to diameter
σ	potential parameter
σ_{HS}	diameter of HS molecular fluid
σ_{LJ}	diameter of LJ molecular fluid

Superscript

$*$	symbol indicating reduced parameter

References

[1] P.T. Cummings, J.E. Denis, Ind. Eng. Chem. Rev. 31 (1992) 1237–1252.
[2] E. Akhmatskaya, B.D. Todd, P.J. Davis, D.J. Evans, K.E. Gubbins, L.A. Pozhar, J. Chem. Phys. 106 (1997) 4684–4695.
[3] I. Bitsanis, J.J. Magda, M. Tirrell, H.T. Davis, J. Chem. Phys. 87 (1987) 1733–1750.
[4] I. Bitsanis, J.J. Magda, M. Tirrell, H.T. Davis, J. Chem. Phys. 89 (1988) 3152–3161.
[5] I. Bitsanis, S.A. Somers, H.T. Davis, M. Tirrell, J. Chem. Phys. 93 (1990) 3427–3431.
[6] B.-J. Zhang, Chem. Phys. Lett. 296 (1998) 266–270.
[7] B.-J. Zhang, Fluid Phase Equilib. 154 (1999) 1–10.
[8] B.-J. Zhang, S.Q. Liang, Y.H. Lu, Fluid Phase Equilib. 180 (2001) 183–194.
[9] H. Zhang, B.-J. Zhang, S.Q. Liang, Y.H. Lu, W.X. Hu, Z.J. Jin, Chem. Phys. Lett. 350 (2001) 247–252.
[10] H. Zhang, B.-J. Zhang, J.W. Lu, S.Q. Liang, Chem. Phys. Lett. 366 (2002) 24–27.
[11] D.M. Heyes, Physica A 146 (1987) 341–359.
[12] D. Nicholson, Carbon 36 (1998) 1511–1523.
[13] D. Nicholson, J. Membr. Sci. 139 (1997) 209–219.
[14] R.F. Cracknell, D. Nicholson, K.E. Gubbins, J. Chem. Soc., Faraday Trans. 91 (1995) 1377–1383.
[15] S. Jost, S. Fritzsche, R. Haberlandt, Chem. Phys. Lett. 279 (1997) 385–388.
[16] E.J. Maginn, A.T. Bell, D.N. Theodorou, J. Phys. Chem. 97 (1993) 4173–4181.
[17] J. Naghizadeh, S.A. Rice, J. Chem. Phys. 36 (1961) 2710–2720.
[18] J.P.J. Michels, N.J. Trappeniers, Chem. Phys. 33 (1975) 195–200.
[19] G. Jacucci, I.R. Mcdonald, Physica A 80 (1975) 607–625.
[20] A.D. John, Lange's Handbook of Chemistry, McGraw-Hill, New York, 1999.